

29 **Abstract**

30 Manganese (Mn) is an essential trace element required for optimal functioning of cellular biochemical pathways in
31 the central nervous system. Elevated exposure to Mn through environmental and occupational exposure can cause
32 neurotoxic effects resulting in manganism, a condition with clinical symptoms identical to idiopathic Parkinson's
33 disease. Epigenetics is now recognized as a biological mechanism involved in the etiology of various diseases. Here,
34 we investigated the role of DNA methylation alterations induced by chronic Mn (100µM) exposure in human
35 neuroblastoma (SH-SY5Y) cells in relevance to Parkinson's disease. A combined analysis of DNA methylation and
36 gene expression data for Parkinson's disease associated genes was carried out. Whole genome bisulfite conversion
37 and sequencing (WGBS) indicates epigenetic perturbation of key genes involved in biological processes associated
38 with neuronal cell health. Integration of DNA methylation data with gene expression reveals
39 epigenetic alterations to *PINK1*, *PARK2* and *TH*, genes that play critical roles in the onset of Parkinsonism. The present
40 study suggests that Mn-induced alteration of DNA methylation of *PINK1-PARK2* may influence mitochondrial
41 function and promote Parkinsonism. Our findings provide a basis to further explore and validate the epigenetic basis
42 of Mn induced neurotoxicity.

43 **Keywords:** DNA methylation, Manganese, Epigenetics, Parkinson's disease, WGBS

44 **Abbreviations:**

45	APC	-	Adenomatous polyposis coli
46	ATP2B2	-	ATPase Plasma Membrane Ca ²⁺ Transporting 2
47	CXXC1	-	DNA-Binding Protein With PHD Finger And CXXC Domain
48	DLK1	-	Delta-Like 1 Homolog (Drosophila)
49	DRD2	-	Dopamine receptor D2
50	GBE1	-	1,4-alpha-glucan-branching enzyme
51	Mn	-	Manganese
52	NRXN3	-	Neurexin 3
53	NSF	-	N-Ethylmaleimide Sensitive Factor
54	PAN2	-	Poly(A) Specific Ribonuclease Subunit
55	PARK2	-	Parkin RBR E3 Ubiquitin Protein Ligase
56	PINK1	-	PTEN-induced putative kinase 1
57	PPI	-	Protein Protein Interaction
58	SLC25A4	-	Solute Carrier Family 25 Member 4
59	SNCA	-	Synuclein Alpha
60	STUB1	-	STIP1 Homology And U-Box Containing Protein 1
61	TH	-	Tyrosine Hydroxylase
62	VDAC	-	Voltage-dependent anion-selective channel protein 1
63	WGBS	-	Whole genome bisulfite conversion and sequencing
64	YWHAZ	-	Tyrosine 3-Monooxygenase/Tryptophan 5-Monooxygenase Activation Protein Zeta

65

66 1. Introduction

67 Manganese (Mn) is naturally present in the environment and is a vital trace element required for proper functioning
68 of cellular biochemical pathways. Although Mn is essential for human physiology, elevated exposure can elicit
69 neurotoxic effects on the developing central nervous system (CNS) (Erikson et al. 2007; Tamm et al. 2008). Miners
70 and workers of ferroalloy, smelting and metallurgy industries are occupational populations exposed to manganese
71 (Finkelstein MM 2007; Lucas et al. 2015). Manganese containing pesticide formulations such as asmaneb and paraquat
72 are used in agriculture to treat various plant pathologies (Roede et al. 2011). Methylcyclopentadienyl manganese
73 tricarbonyl (MMT) used as a petrol anti-knock additive also releases Mn as a combustion product in the atmosphere
74 (Crump 2000). Recently high exposure to Mn has been reported to occur with use of psychoactive stimulants in
75 recreational drugs (de Bie et al. 2007). The concentration of Mn in drinking water also was found to exceed the WHO
76 regulatory standard (400 µg/L) (WHO 2006). Significant levels of Mn have been detected in children hair samples
77 and breast milk in populations residing in the vicinity of industrial steel plant (Sharma R. 2005). Therefore, the main
78 paths of environmental exposure to Mn in the general population occur through intake of contaminated drinking water,
79 dietary foods and inhalation of ambient air with elevated level of manganese (Roede et al. 2011; ATSDR 2012).

80 High occupational and environmental exposure to Mn has been reported to cause manganism, a condition with
81 neurological symptoms similar to those of idiopathic Parkinson's disease (Settivari et al. 2013). Clinically, the
82 symptom includes tremors, bradykinesia, rigidity, postural instability and facial muscle spasms. The low chronic level
83 of exposure to Mn for prolonged period have been found to be associated with elevated risk of developing
84 Parkinson's disease (Gorell et al. 2004).

85 Parkinson's disease is characterized by the progressive loss of dopaminergic neurons in substantia nigra pars
86 compacta (SNpc) with subsequent depletion of dopamine, impairing the execution of coordinated movements
87 (Anumantha et al. 2012). Recent evidence suggest that Mn deposition occurs in substantia nigra region and hence may
88 be postulated to be associated with the etiology of Parkinson's disease (Park et al. 2007).

89 Epigenetics entails the study of heritable changes in gene expression that occur independent of modifications to
90 nucleotide sequences (Schnekenburger M 2007). Control of gene expression is essential for normal physiological
91 functioning of cell and the epigenetic machinery has an important role in regulating these processes. Epigenetic
92 regulation includes of DNA methylation, histone modifications and miRNA expression. The involvement of
93 epigenetic deregulation in the cause of various neurodegenerative disorders such as Parkinson's, Huntington
94 Alzheimer and other mood disorders has been suggested (Migliore L 2009). Environmental toxicants that induce
95 epigenetic alterations have been implicated in the susceptibility and progression of environmentally mediated chronic
96 diseases (Baccarelli and V. Bollati 2009; Anumantha et al. 2012).

97 The generation of oxidative stress through mitochondrial accumulation of Mn and subsequent mitochondrial
98 respiratory dysfunction is thought to be primarily responsible for neurotoxic effects of manganese (McCubrey JA and
99 Lahair MM 2006). For example, Mn has been reported to cause apoptotic cell death via oxidative stress in the human
100 neuroblastoma SH-SY5Y cell line (Stephenson et al. 2013). Exposure to heavy metals such as As, Pb, Cd and Ni

101 generates reactive oxygen species that may alter the level of DNA methylation in rat and other animal
102 models(Martinez R 2011).

103 DNA methylation alterations occur primarily at CpG sites through addition of a methyl group to the 5' position of
104 cytosines. Around 70% of the CpGs sites are constitutively methylated in human genome, while unmethylatedCpGs
105 are generally located in CpG islands associated with promoter regions of genes (Martin C 2007). Methylation
106 modifications at CpG sites can induce conformational changes to chromatin and thereby modulate accessibility of
107 gene promoter regions to the transcription machinery (Orphanides G 2002).

108 Human population is inevitably exposed to manganese in the environmental and occupational settings. It is evident
109 from the epidemiological studies and available literature that populations exposed to low chronic levels of Mn have a
110 propensity to develop idiopathic Parkinson's disease (Kim et al. 2002). However, the hypothesis involving the
111 potential role of epigenetic mechanisms in manganese induced neurotoxicity has not been explored (Tarale et al.
112 2016).

113 In the present study we investigated the impact of chronic Mn exposure on whole genome DNA methylation levels
114 and profiling of differentially methylated genes. We used the dopaminergic human neuroblastoma (SH-SY5Y) cell
115 line as a model to explore the role of DNA methylation alterations induced by Mn and its possible association
116 withParkinson's disease. In support of our DNA methylation data, we also correlated differentially methylated
117 regions with expression levels ofParkinson's disease associated genes. The results of the present investigation provide
118 insight how epigenetic mechanisms may promote manganese-induced idiopathic Parkinson's disease.

119

120 **2. Material and Methods**

121 **2.1 Cell line**

122 Human neuroblastoma (SH-SY5Y) cell line was procured from National Center for Cell Science (NCCS),
123 Pune, India. Cells were grown in Ham's F-12 medium supplemented with 10% fetal bovine serum, 100 U/mL
124 penicillin, 50 µg/mL streptomycin, and 25 µg/mL Fungizone. Cells were maintained at 37°C in a humidified
125 atmosphere with 5% CO₂.

126 **2.2 Chronic Mn²⁺ exposure**

127 SH-SY5Y cells were seeded in 25mm² flask (5 x10⁵ cells/ml) and grown up to 70% confluence level. After
128 achieving the 70% confluence level, cells were exposed to 100 µM of Mn²⁺ in the form of MnCl₂ (Sigma Aldrich,
129 USA). The dose of Mn²⁺for exposure in this study was selected based on the published research articles and
130 preliminary studies (Bornhorst et al. 2013; Stephenson et al. 2013). Chronic exposure of Mn²⁺was given for the
131 period 30 days, three controls and three exposed flask were maintained during the period of exposure. Medium was
132 subsequently changed at every third day and after each passage throughout the exposure period. Cells were treated
133 with Mn²⁺after each passage as the cells get adhere to the flask.

134 **2.3 Whole-genome (DNA) methylation sequencing and data processing**

135 At the end of exposure period, cells were harvested for the whole genome DNA methylation sequencing
136 and analysis as follows.

137 **2.3.1 Isolation of genomic DNA**

138 SH-SY5Y cells were harvested and suspended in lysis buffer (500µl of TNE buffer, 25 µl of 20% sodium
139 dodecyl sulfate (SDS), 7.5 µl of proteinase K (20mg/ml)). Samples were then incubated at 37°C for 3 hrs. After 3 h
140 incubation, 250µl of phenol: chloroform: isoamyl alcohol (25:24:1) was added to cell lysate and mixed well, further
141 samples were kept for 30 min at room temperature. Later samples were centrifuged at 14000g for 15 min. After
142 centrifugation aqueous layer was collected to new eppendorf tubes and DNA was precipitated with 90% ethanol and
143 25µl of 0.3 M sodium acetate. Samples were centrifuged at 14000g for 10 min to pellet out the precipitated DNA.
144 Precipitated DNA was washed with 70% ethanol and again re-centrifuged. Finally DNA was air dried and re-
145 suspended in DNase free water. Quantification of genomic DNA was carried out using
146 ND8000Nanodropspectrophotometer.

147 **2.3.2 Bisulfite conversion**

148 EZ DNA Methylation Gold™ Kit (Zymo Research) was used for the bisulfite conversion of 20µl
149 (200ng/µl) of genomic DNA. 20µl of each DNA sample was mixed with 130µl of CT conversion reagent and
150 programmed at thermal cycler as; 98° C for 10 min, 64° C for 2.5 hrs, 4° C for 20 hrs. After the incubation, 600µl M
151 binding buffer was added to tubes and transferred to Zymo spin IC column. Columns were centrifuged at 10000g for
152 30 sec. Following centrifugation, columns were washed with M wash buffer. Later 200µl of M desulphonation
153 buffer was added to columns and incubated at room temperature for 20 min followed by centrifugation at max
154 speed. Columns were then washed with M buffer and bisulfite converted genomic DNA was eluted with M elution
155 buffer.

156 **2.3.3 Whole genome bisulfite sequencing**

157 Whole genome bisulfite sequencing was carried out using EpiGnome™ Methyl-Seq Kit on IlluminaHiSeq
158 2500. 100ng of bisulfite converted genomic DNA samples were mixed with 2µl DNA primer and incubated for 5
159 min at 90° C. After the incubation, 4µl of EpiGnome DNA synthesis premix, 0.5µl of 100mM DTT and 0.5µl of
160 EpiGnome polymerase was added to samples and programmed on thermal cycler (25°C for 5 min, 42°C for 30
161 min, 37°C for 2 min). Later 1.0µl of exonuclease was added to each samples and reaction was programmed on
162 thermal cycler (37°C for 10 min, 95°C for 3 min, 25°C for 2min). At the end of programme, 8µl of Terminal Tagging
163 master mix (7.5µl of EpiGnome™ Terminal Tagging premix and 0.5µl DNA polymerase) was added to each sample
164 tubes and programmed on thermal cycler (25°C for 30 min, 95°C for 3 min and hold at 4°C). Prior proceeding DNA
165 library preparation, DNA was purified using AMPure XP system to yield di-tagged DNA. EpiGnome Index PCR
166 Primer kit was used to generate whole genome bisulfite library. To 22.5µl of di-tagged DNA, 24µl of Failsafe PCR
167 premix E, 1.0µl of EpiGnome forward primer, 1.0µl of EpiGnome reverse primer and 0.5µl of Failsafe PCR
168 Enzyme was added and programmed on thermal cycler for 10 cycles as 95°C for 30 seconds, 55°C for 3 min, 68°C

169 and final extension at 68°C for 7 mins. Whole genome bisulfite library was then purified by using AMPure XP
170 system. Total yield of WGB library was quantified using Qubit fluorometer and size distribution of WGB library was
171 analyzed using 2100 bioanalyzer (Agilent). Whole genome bisulfite sequencing (Paired End) of bisulfite library was
172 carried out on Illumina HiSeq 2500 using Illumina SBS and Cluster kit.

173 **2.3.4 Bismark alignment**

174 Whole genome bisulfite sequencing (WGBS) was carried out to generate the DNA methylation map of SH-SY5Y
175 cell line chronically exposed to Mn (100 μM). Two biological replicates, each of control and exposed SH-SY5Y cell
176 line were sequenced. Bismark alignment in control and exposed samples mapped an average of 62% of reads the
177 genome. The 90% of the sequenced data passed Q30 phred quality score. According to Bismark alignment mapping
178 efficiency within a range of 60-68% was considered as the best alignment percentage for reads of >80 base pairs of
179 length. The whole genome bisulfite sequencing (WGBS) data was submitted to National Center for Biotechnology
180 Information (NCBI) Sequence Read Archive (SRA) repository and can be accessed (SRP075314; SRP075316;
181 SRP075243; SRP075313). The publically submitted whole genome DNA methylation data may be further explored
182 using other bioinformatics tools to obtain additional information in relevant to manganese neurotoxicity

183

184 **2.3.5 Methylation analysis and identification of differentially methylated genes**

185 The base calling pipeline (HiSeq Control Software 2.2.38) was used for demultiplexing prior to the
186 generation of fast-q-sequence files, i.e. by separating the libraries according to their indexes. Passed filter (PF) is a
187 cluster that fulfills the default Illumina quality criteria; % of bases (PF) with a quality score greater or equal to 30
188 was used as a cutoff to remove sequences produced from clusters with low signal to noise ratio (e.g. overlapping
189 DNA clusters). A 6-8 bp pair DNA sequence tag found in adaptor sequence to uniquely identify each library; used at
190 demultiplexing step. This filtered reads are aligned to the Human Genome reference (hg19/GRCH37 Assembly).
191 Bismark tool (Version – V 0.10.1) was used for the alignment of bisulfite converted genome sequences. Each
192 cytosine (C) present in raw reads was extracted from alignment output file (SAM file) using Bismark. The position
193 of every cytosine (C), depending on cytosine (C) context (CpG, CHC and CHH) methylated cytosine (C) was
194 labeled as “+” (forward read) while unmethylated cytosine (C) labeled as “-” (reversed read). Every methylated
195 cytosine (C) was annotated against human reference genome using Varimat tool. Each cytosine (C) was tracked to
196 its original location in the genome based on its chromosome position to identify differentially methylated regions.
197 Methylation difference between control and Mn²⁺ exposed cells was calculated by using DMAP (Differential
198 Methylation Analysis Package for RRBS and WGBS data). We screened for differentially methylated genes
199 between Control and Mn-treated samples having methylation difference above 0.1 (hyper or hypomethylation). The
200 Database for Annotation, Visualization and Integrated Discovery (DAVID) version 6.7 (<https://david.ncifcrf.gov/>)
201 was used for functional annotation clustering of differentially methylated genes.

202 **2.4 Gene expression profiling for Parkinson’s disease associated genes**

203 SH-SY5Y cells were harvested at the end of exposure period for the isolation of total RNA. Trizol reagent
204 (Invitrogen) was used for the isolation of total RNA. Quantification of total RNA was carried out using NanoDrop
205 8000 spectrophotometer. 2000ng of RNA was converted to cDNA using the RT² first strand kit (Qiagen, Germany)
206 as per the manufacturer instructions. The Human Parkinson's Disease RT² Profiler PCR Array (Qiagen, Germany)
207 profiles the expression of 84 key genes directly or potentially involved in Parkinson's disease . Each RT² Profiler
208 PCR array contains 12 controls that were used for the normalization of RT-PCR results. Applied Biosystems7300
209 real time PCR was used for the relative quantification and RT-PCR was performed as per the manufacturer protocol.
210 $\Delta\Delta C_t$ method of relative quantification was used for the calculation of fold change and interpretation of control
211 wells.

212 3. Results

213 3.1 Methylation profiling

214 We scanned the genome of Mn-treated and untreated SH-SY5Y cells for cytosine methylation by mapping
215 methylated and unmethylated cytosines to a virtual, bisulfite converted human genome. Chronic exposure to
216 manganese resulted in overall slight increase in the percentage of methylation density at CpG sites from 70.4%to
217 73.6%(Figure 1A and B). Methylation of cytosines has also been detected at non-CpG sites in neuronal DNA (Ryan
218 Lister, Eran A. Mukamel, Joseph R. Nery, Mark Urich et al. 2013). We therefore, examined our WGBS data setsfor
219 the presence ofmethylation events at CHG and CHH sites(H = A/C/T). In context of non-CpG sites anincrease in
220 methylation levels was detectedat CHG sites,from 3.4% to 19.7%(Figure 1C). Similarly,at CHH sites, methylation
221 was markedly elevated, from 3.7%to 25.4%(Figure 1D).

222 The expression of genes is influenced by cytosine modifications. To map transcriptional start sites (TSS) and to
223 identify genes associated with TSS regionson their original locations in chromosomes, we used VariMAT to
224 annotate the observed cytosine methylation events. This gives the list of differentially methylated genes that are
225 linked with altered state of CpG methylation.

226 3.2 Differentially methylated gene analysis

227 We examined if a genome-wide trend for methylation of TSS could be detected. Methylation densities of
228 CpG sites within 5 kilobase (kb) regions upstream and downstream of TSS were determined with 200 base pair (bp)
229 genomic bins using our WGBS data. This analysis suggested a subtle trend towards methylated TSS and increased
230 levels of cytosine modification downstream, in the gene bodies of the Mn exposed samples (Supplementary figure
231 2).The WGBS data were further analyzed for identification of genomic sequences associated with a distinct CpG
232 methylation status. Chromosome wise analysis identified 24868 differentially methylated genes. Genes from this list
233 were further shortlisted based on the p_value (<0.05) to obtain a list of around 10213 differentially methylated genes
234 at statistically significant level (Supplementary file 1). The list of genes was again screened, based on <0.1%
235 methylation difference/change, yielding 6846 differentially methylated regions of genes. The heat map showing the
236 differential methylation status for genes with >0.1methylation difference is given in supplementary figure S1.The

237 Database for Annotation, Visualization and Integrated Discovery (DAVID) v6.7 was used for functional annotation
238 clustering of differentially methylated genes. The hypermethylated and hypomethylated genes were separately
239 analyzed using the DAVID database for functional annotation and clustering. DAVID based analysis shows that the
240 hypermethylated genes are involved in metal ion binding (25%), cytoskeleton (16%), chromatin modification (12%),
241 regulation of transcription (7%), apoptosis and iron binding (13%) (Figure 2A). The hypomethylated genes are
242 involved in regulation of signal transduction (38%), transcription (15%), neuron differentiation and development
243 (5%), synaptic transmission and MAPK signaling pathways (9%) (Figure 2B). The important hypermethylated genes
244 regulating the synaptic transmission are PINK1, PARK2, SMAD7, VGF, DBH, GDNF, TH, GRIK3, and NGF. The
245 genes responsible for regulating the apoptosis such as MGMT, CASP3, CARD14, MAPK8, MAP3K7, NGFR,
246 YWHAZ were also found to be hypermethylated. The several inflammatory genes, including HRH1, IGF2, ITGB6,
247 MAP2K3, YWHAZ, LYN and MASP1 were found to be hypomethylated. In summary, DAVID analysis reveals that
248 manganese exposure alters the DNA methylation status of genes involved in the important biological pathways. The
249 perturbation in the regulation of biological pathways via methylation alteration of associated genes may be
250 responsible for the neurotoxic mechanism of manganese.

251

252 **3.3 Correlation of differentially methylated genes with known genes in Parkinson's disease RT² Profiler** 253 **array**

254 The DNA methylation profiling approach identifies genes potentially involved in pathways related to Parkinson's
255 disease. In order to correlate and validate the differentially methylated genes with their relative level of gene
256 expression, we used the Human Parkinson's Disease RT² Profiler PCR Array (Qiagen, Germany). From a total of 84
257 genes screened with this PCR array, we found that 34 genes had significantly diminished expression levels ($p < 0.05$)
258 in the Mn treated SH-SY5Y cells. To assess if this set of down-regulated genes is enriched for certain functional
259 pathways or networks, the DAVID database was used for annotation and clustering based on the gene ontology. The
260 identified 34 genes were found to be involved in three biological pathways, including neuronal development and
261 differentiation (17 genes), dopamine metabolic process (8 genes), and ubiquitin mediated proteolysis (5 genes)
262 (Figure 3). Important genes associated with these pathways are ATP2B2, DRD2, NRXN3, SLC25A4, SNCA, TH,
263 VDAC, PARK2, PINK1, NSF, PAN2, STUB1. These three pathways are known to play a role in the pathology of
264 Parkinson's disease. The same pathways that we identified to be deregulated using the RT² expression profiler were
265 also flagged by a DAVID analysis of our list of differentially methylated genes. The differentially methylated genes
266 identified in the WGBS screen were compared to the list of 34 genes identified in the RT² PCR expression profiler
267 array for human Parkinson's disease and additionally with genes that have been reported in the literature to be
268 associated with Parkinson's disease. This type of comparison could indicate a probable connection between
269 manganese induced DNA methylation alteration and changes in expression of Parkinson's disease associated genes.
270 Based on this analysis we identified 119 differentially methylated genes from our WGBS data set, which is shown in
271 a heat map (Figure 4).

272 Correlation of DNA methylation and gene expression in the present study identifies 10 genes in relevance to
273 Parkinson's disease (APC, ATP2B2, CXXC1, DLK1, GBE1, NSF, PARK2, PINK1, TH, and YWHAZ) (Figure 5).
274 Among these 10 genes; TH, PARK2 and PINK1 are particularly recognized as important players in the etiology of
275 Parkinson's disease as they have a significant role in the proteosomal degradation, protein kinase activity and
276 dopamine biosynthesis (Satake et al. 2009) Table 1 gives the list of 10 genes with their status in DNA methylation
277 profile and RT² PCR gene expression analysis. The methylation alteration of these critical genes shows the probable
278 association between manganese exposure and Parkinson's disease at an epigenetic level. The STRING database
279 (Search Tool for the Retrieval of Interacting Genes/Proteins) is mainly devoted to documenting known and predicted
280 functional protein-protein interactions. Our STRING analysis reveals a significant biological association between
281 the genes as group with PPI (p-value<0.0002) (Figure 6). The major biological process (GO) altered in connection
282 to Parkinson's disease has been highlighted in the figure 6.

283

284 4. Discussion

285 Epigenetics has gained recognition as a biological mechanism that is associated with the manifestation of
286 various human diseases. The interaction between gene and environment is thought to be, in part at least, mediated
287 via epigenetic mechanisms. Epigenetic changes have already been implicated in certain cases of Parkinson's disease
288 (Moyano et al. 2011). There is growing evidence suggesting a link between manganese exposure and Parkinson's
289 disease (Racette et al. 2012). However there are limited studies that aimed to determine the connection between
290 manganese exposure with deregulation in epigenetic mechanisms leading to Parkinson's disease (Nannan et al.
291 2016).

292 The human neuroblastoma cell line (SH-SY5Y) has been used as *ex vivo* cell model to investigate the neurotoxic
293 mechanism of manganese (Li et al. 2010). In the present study we chronically exposed a neuroblastoma cell line to
294 Mn²⁺ (100µM) for a period of 30 days, followed by WGBS and gene expression analysis for Parkinson's disease
295 associated genes. Hypermethylation of CpG sites within gene promoter regions generally correlates with repression
296 of gene expression (Nan et al., 1998). In contrast, non-CpG cytosine modifications have been detected in active
297 genomic regions in human and mouse brain (Lister et al. 2013; Guo et al. 2014). In the present study we observed an
298 increase of non-CpG methylation, particularly at CHH sites (figure 1C and 1D). The methyl CpG binding protein 2
299 (MECP2) plays an essential role in normal neuronal development (Chahrour et al. 2009) and appears to
300 modulate transcription by interaction with both methylated CpG sites and methylated mC sites (Matthew et al.
301 2013). The overall methylation increase at both CpG and non-CpG sites observed in the present study may be
302 associated with an altered distribution of MECP2.

303 The WGBS data was further analyzed to identify specific genes with altered methylation. The list of significantly
304 hypermethylated and hypomethylated genes was submitted to Database for Annotation, Visualization and Integrated
305 Discovery (DAVID) for functional annotation and clustering (Dennis et al. 2003). DAVID analysis indicates the
306 involvement of these differentially methylated genes in multiple important biological pathways such as regulation of

307 neuronal differentiation and development, synaptic transmission, signal transduction, inflammation and programmed
308 cell death. Exposure to manganese has been reported to alter the DNA methylation status of various CpG loci during
309 the neurodevelopmental process (Maccani et al. 2015). The hypomethylation of inflammatory nitric oxide synthase
310 gene (iNOS) was reported responsible for elevated signs of Parkinsonism among the Mn miners (Susan et al. 2014).
311 DAVID based functional classification of genes in the present work also identifies the hypomethylation of
312 inflammatory genes.

313 It is important to recognize there may not be a direct correlation between the DNA methylation status and
314 expression profile of genes (Jones 2012). Hence it becomes important to integrate DNA methylation data with gene
315 expression profiles. In the recent study combined analysis of gene expression in addition to the DNA methylation
316 was carried out for a select number of genes. DAVID analysis identifies neuronal development, synaptic
317 transmission and apoptosis as common pathways involved in Mn induced Parkinsonism.

318 Clinically, Parkinson's disease is accompanied by motor dysfunction because of dopamine depletion occurring as a
319 result of dopaminergic neuronal degeneration within the substantianigra pars compacta (SNpc) (Ammal Kaidery et
320 al. 2013).Five genetic loci, including α -synuclein, parkin, PINK1, DJ-1, and LRRK2 are the most extensively
321 studied and considered as critical risk factors for the onset of sporadic Parkinson's disease (Rochet and Hay 2012).
322 In the present study activity of two genetic loci, parkin and PINK1 was found to be altered via hypermethylation
323 upon manganese exposure.

324 Tyrosine hydroxylase (TH) has an important role in dopamine biosynthesis. Mn exposure has been found to alter the
325 activity of TH, both in dopaminergic neuronal cells and a Zebrafish model of manganese (Zhang et al. 2011;
326 Bakthavatsalam et al. 2014). The result of the present investigation suggests that cytosine methylation plays a role in
327 modulating TH gene activity and may contribute to diminished expression levels, which is in agreement with
328 previous studies on Mn neurotoxicity (Bakthavatsalam et al. 2014).. However, our results require further validation
329 and testing in other animal models.

330 Parkin/PARK2 is an autosomal recessive gene and mutations in one of the alleles has been shown to cause the
331 clinical features of Parkinsonism and as risk factor for early onset of Parkinson's disease (EOPD) (Periquet M et al.
332 2003; Padmaja et al.2012)The present study suggests that hypermethylation of PARK2 with subsequent reduction in
333 gene expression may be another molecular mechanism that potentiates Mn toxicity via loss of control over Divalent
334 Metal Transporter (DMT1) mediated Mn transport(Roth and Garrick 2003; Higashi et al. 2004).

335 PINK1 is a serine/threonine kinase with neuroprotective function that localizes to mitochondria (Petit et al. 2005;
336 Silvestri et al. 2005). We found PINK1 expression to be decreased in the present study, presumably through
337 hypermethylation of the gene. Perturbation in PINK1 function through mutation has been reported to cause
338 impairment of mitochondrial function, synaptic transmission and elevated sensitivity to oxidative stress (Kitada et
339 al. 2008). PINK1 has also been found to interact with polycomb histone-methylation modulator (EED/WAIT1) and
340 regulate gene expression during SH-SY5Y differentiation (Berthier et al. 2013).

341 PARK2 and PINK1 have been identified as key genes responsible for early onset of Parkinsonism via loss of
342 mitochondrial quality control (Noriyuki Matsuda 2015). Mitochondrial quality control is an essential function of
343 healthy neurons ensuring cell survival, while dysfunction of complex I has been reported to induce Parkinsonism
344 and sporadic Parkinson's disease (Schapira 2008). Parkin/PARK2 is selectively targeted to depolarized
345 mitochondria to facilitate the removal of damaged mitochondria through ubiquitination of outer mitochondrial
346 substrate (Narendra et al. 2010). PINK1 kinase activity is responsible for both activation and recruitment of PARK2
347 to mitochondrial membrane (Youle 2014). Initially, PINK1 phosphorylate ubiquitin on depolarized mitochondria
348 that function as an activator of PARK2 activity through repression of auto-inhibiting activity of PARK2 (Trempe et
349 al. 2013). The subsequent events of ubiquitin-phosphorylation act as a signal for PINK1-PARK2 mediated
350 mitophagy based removal of depolarized mitochondria (De-Chen et al. 2015). The findings suggest that PINK1-
351 PARK2 together have a vital role in regulating mitochondrial quality control and thereby appear to prevent the onset
352 of Parkinsonism (Narendra, et at. 2012; Youle 2014). DNA methylation studies in manganese exposed mouse model
353 recently reported alteration to several mitochondrial genes (Yang et al. 2016). Epigenetic down-regulation of both
354 PINK1-PARK2 through hypermethylation in the present study supports the previous findings and supports the
355 concept that mitochondrial dysfunction might be responsible for Mn induced Parkinsonism.

356 This is one of the first studies to reveal manganese induced alterations in DNA methylation. The results indicate the
357 influence of chronic manganese exposure on epigenetic de-regulation of Parkinson's disease associated pathways.
358 Our data, along with those communicated by Yang and colleagues (Yang et al. 2016) signify the importance of
359 considering the role of epigenetic mechanisms in Mn induced neurotoxic effects. These results require validation
360 and replication in other animal models of Parkinson's disease.

361

362 **5. Conclusion**

363 The study shows that chronic manganese exposure on dopaminergic human neuroblastoma cells (SH-SY5Y) induces
364 global alteration to DNA methylation levels of genes involved in biological pathways, including neuronal
365 development and differentiation, synaptic transmission, signal transduction, and inflammation. Mitochondrial
366 dysfunction is known to be involved in Parkinsonism and Mn has also been shown to alter mitochondrial function.
367 The present study suggests an epigenetic alteration of PINK1-PARK2 which might contribute to the Mn mediated
368 mitochondrial dysfunction and probably in the etiology of Parkinson's disease. A better understanding of Mn
369 induced neurotoxicity and an altered epigenetic landscape that comes along with Mn exposure could lead to the
370 identification of new prognostic and therapeutic epigenetic targets.

371

372

373

374

375 **Figure legends**

376 **Figure 1.** Overall methylation densities (%) from the single-base resolution methylomes (WGBS data) were
377 determined for (A) cytosines at CpG sites and (B) cytosines at non-CpG sites. Non-CpG methylation of cytosines is
378 categorized in the context of CHG and CHH sequences, where H = A/C/T. The frequencies of these cytosine
379 methylation events for different CHG and CHH sequence combinations is shown for the control (C) and the
380 manganese-treated sample (D). The WGBS approach generates sequence data for both, the reference sequence of the
381 genome ('Watson' DNA strand) and the sequence of the complementary DNA strand ('Crick' DNA strand).
382 Methylation densities do not show any obvious strand bias.

383 **Figure 2.** DAVID database was used for the Gene Ontology (GO) functional annotation cluster analysis. The figure
384 depicts the major biological pathways associated with (A) Hypermethylated and (B) Hypomethylated genes.

385 **Figure 3.** Gene Ontology (GO) functional annotation cluster analysis was performed using DAVID database for
386 differentially expressed genes identified in PCR array for Human Parkinson's Disease.

387 **Figure 4.** Heatmap clustering of 119 genes screened based on involvement in Parkinson's disease pathways. Red and
388 green colors represent the high and low level of DNA methylation.

389 **Figure 5.** Relative gene expression level of the selected genes in Human Parkinson's Disease RT² Profiler PCR
390 Array. Error bar represent the standard error (SE) and * indicates statistical significance ($p < 0.05$).

391 **Figure 6.** The STRING database (Search Tool for the Retrieval of Interacting Genes/Proteins) based analysis shows
392 the functional association between the genes. Protein-protein interaction (PPI) enrichment p-value, highlighted in
393 blue box indicates significant interaction and biological association between genes as a group. Biological process
394 (GO) and genes in network highlighted in red box represent the process deregulated in Parkinson's disease pathway.

395 **Table 1.** Table depicting the genes identified on correlation between genes in DNA methylation and RT² profiler
396 array for Parkinson's disease. Table shows the biological function of the genes listed

397 **Conflict of Interest**

398 The authors declare that there is no conflict of interests regarding the publication of this paper.

399

400 **Acknowledgement**

401 The authors are thankful to CSIR-NEERI, Nagpur, India for providing the necessary facilities. Authors are grateful
402 to Integrated NextGen approaches in health, disease and environmental toxicity (INDEPTH) Networking project
403 (BSC 0111) for providing necessary funding. Institutional Knowledge Resource Center (KRC) No.
404 KRC/2016/SEP/EHD/2.

405 **References**

- 406 Ammal Kaidery N, Tarannum S TB (2013) Epigenetic Landscape of Parkinson's Disease: Emerging Role in Disease
407 Mechanisms and Therapeutic Modalities. *Neurotherapeutics* 10:698–708. doi: DOI 10.1007/s13311-013-
408 0211-8
- 409 Anumantha Kanthasamy, Huajun Jina, Vellareddy Anantharama GS, Velusamy Rangasamyb, Ajay Ranab AK
410 (2012) Emerging Neurotoxic Mechanisms in Environmental Factors Induced Neurodegeneration.
411 *Neurotoxicology* 33:833–837. doi: doi:10.1016/j.neuro.2012.01.011.
- 412 ATSDR (2012) Toxicological Profile for Manganese.
- 413 Baccarelli and V. Bollati (2009) Epigenetics and environmental chemicals. *Curr Opin Pediatr* 21:243–251.
- 414 Bakthavatsalam S, Sharma SD, Sonawane M , Thirumalai V DA (2014) A zebrafish model of manganism reveals
415 reversible and treatable symptoms that are independent of neurotoxicity. *Dis Model Mech* 7:1239–1251. doi:
416 doi:10.1242/dmm.016683
- 417 Berthier A, Jimenez-Sainz J PR (2013) PINK1 regulates histone H3 trimethylation and gene expression by
418 interaction with the polycomb protein EED/WAIT1. *Proc Natl Acad Sci USA* 110:14729–14734.
- 419 Bornhorst J, Meyer S, Weber T, Boker C, Marschal T, Mangerich A, Beneke S BA and ST (2013) Molecular
420 mechanisms of Mn induced neurotoxicity: RONS generation, genotoxicity, and DNA-damage response. *Mol*
421 *Nutr Food Res* 57:1255–1269.
- 422 Chahrour M, Sung Yun Jung, Chad Shaw, Xiaobo Zhou, Stephen T. C. Wong, JunQin HYZ (2009) MeCP2, a Key
423 Contributor to Neurological Disease, Activates and Represses Transcription. *Science* (80-) 320:1224–1229.
- 424 Crump KS (2000) Manganese exposures in Toronto during use of the gasoline additive, methylcyclopentadienyl
425 manganese tricarbonyl. *J Expo Anal Env Epidemiol* 10:227–239.
- 426 D RJA and GM (2003) Iron interactions and other biological reactions mediating the physiological and toxic actions
427 of manganese. *Biochem Pharmacol* 66:1–13.
- 428 de Bie, R. M., Gladstone, R. M., Strafella, A. P., Ko, J. H., and Lang AE (2007) Manganese-Induced Parkinsonism
429 Associated With Methcathinone (Ephedrone) Abuse. *Arch Neurol* 64:886–889.
- 430 De-Chen Lin, Liang Xu, Ye Chen, Haiyan Yan, Masaharu Hazawa, Ngan Doan, Jonathan W. Said, Ling-Wen Ding,
431 Li-Zhen Liu, Henry Yang, Shizhu Yu, Michael Kahn, Dong Yin and HPK (2015) Genomic and Functional
432 Analysis of the E3 Ligase PARK2 in Glioma. *Cancer Res* 75:CAN-14-1433. doi: doi: 10.1158/0008-5472
- 433 Dennis G Jr, Sherman BT, Hosack DA, Yang J, Gao W, Lane HC LR (2003) DAVID: Database for Annotation,
434 Visualization, and Integrated Discovery. *Genome Biol* 4:P3.
- 435 Erikson K. M, Thompson K AJ and AM (2007) Manganese neurotoxicity: A focus on the neonate. *Pharmacol Ther*
436 113:369–377.
- 437 Finkelstein MM JM (2007) A study of the relationships between Parkinson's disease and markers of traffic-derived
438 and environmental manganese air pollution in two Canadian cities. *Env Res* 104:420–432.
- 439 Gautier CA, Kitada T SJ (2008) Loss of PINK1 causes mitochondrial functional defects and increased sensitivity to
440 oxidative stress. *Proc Natl Sci USA* 105:11364–11369.
- 441 Gorell JM, Peterson EL, Rybicki BA JC (2004) Multiple risk factors for Parkinson's disease. *J NeurolSci* 217:169–
442 174.
- 443 Guo JU, Su Y, Shin JH, Shin J, Li H, Xie B, Zhong C, Hu S, Le T, Fan G, Zhu H, Chang Q, Gao Y, Ming GL SH
444 (2014) Distribution, recognition and regulation of non-CpG methylation in the adult mammalian brain. *Nat*

445 Neurosci 17:215–222.

446 Higashi Y., Asanuma M., Miyazaki I., Hattori N. MY and ON (2004) Parkin attenuates manganese-induced
447 dopaminergic cell death. *J Neurochem* 89:1490–1497.

448 Kim, Y., Kim, J. M., Kim, J. W., Yoo, C. I., Lee, C. R., Lee JH (2002) Dopamine transporter density is decreased in
449 Parkinsonian patients with a history of manganese exposure: What does it mean? *Mov Disord* 17:568–575.

450 Kitada T, Pisani A, Porter DR, Yamaguchi H, Tscherter A, Martella G, Bonsi P, Zhang C, Pothos EN SJ (2007)
451 Impaired dopamine release and synaptic plasticity in the striatum of PINK1-deficient mice. *Proc Natl Acad*
452 *Sci USA* 104:11441–11446.

453 Li Y, Sun L, Cai T, Zhang Y, Lv S WY (2010) α -Synuclein overexpression during manganese-induced apoptosis in
454 SH-SY5Y neuroblastoma cells. *Brain Res Bull* 81:428–433.

455 Lister R, Mukamel EA, Nery JR, Urich M, Puddifoot CA, Johnson ND, Lucero J, Huang Y, Dwork AJ, Schultz
456 MD, Yu M, Tonti-Filippini J, Heyn H, Hu S, Wu JC, Rao A, Esteller M, He C, Haghghi FG, Sejnowski TJ,
457 Behrens MM EJ (2013) Global epigenomic reconfiguration during mammalian brain development. *Science*
458 (80-). doi: doi: 10.1126/science.1237905.

459 Lucas E.L., Bertrand P., Guazzetti S., Donna F., Peli M., Tjursa.P. LR, D.R. S (2015) Impact of ferromanganese
460 alloy plants on household dust manganese levels: Implications for childhood exposure. *Environ Res* 138:279–
461 290.

462 Maccani JZ, Koestler DC, Houseman EA, Armstrong DA, Marsit CJ KK (2015) DNA methylation changes in the
463 placenta are associated with fetal manganese exposure. *Reprod Toxicol* 47:43–49. doi: doi:
464 10.1016/j.reprotox.2015.05.002. Epub 2015 May 15.

465 Martin C ZY (2007) Mechanisms of epigenetic inheritance. *Cell Biol* 19:266–272.

466 Martinez R CH (2011) Environmental epigenetics in metal exposure. *Epigenetics* 6:820–827.

467 Matthew J Lyst, Robert Ekiert, Daniel H Ebert, Cara Merusi, Jakub Nowak, Jim Selfridge, Jacky Guy, Nathaniel R
468 Kastan, Nathaniel D Robinson, Flavia de Lima Alves, Juri Rappsilber MEG& AB (2013) Rett syndrome
469 mutations abolish the interaction of MeCP2 with the NCoR/SMRT co-repressor. *Nat Neurosci* 17:898–902.

470 McCubrey JA, Lahair MM FR (2006) Reactive oxygen species-induced activation of the MAP kinase signaling
471 pathways. *Antioxid Redox Signal* 8:1775–1789.

472 Migliore L CF (2009) Environmental-induced oxidative stress in neurodegenerative disorders and aging. *Mutat Res*
473 674:73–84.

474 Moyano EM, Pora S, Escaramis G, Rabionnet R, Iraola S, Kagerbauer B, Parrilla YE, Ferrer I EX and M EL (2011)
475 MicroRNA profiling of Parkinson’s disease brains identifies early downregulation of miR-34b/c which
476 modulate mitochondrial function. *Hum Mol Genet* 20:3067–3078. doi: doi:10.1093/hmg/ddr210

477 Nan X, H.-H. Ng CAJ et al (1998) Transcriptional repression by the methyl-CpG-binding protein MeCP2 involves a
478 histone deacetylase complex. *Nature* 393:386–389.

479 Narendra, D., Walker, J.E., and Youle R (2012) Mitochondrial quality control mediated by PINK1 and Parkin: links
480 to parkinsonism. *Cold Spring Harb Perspect Biol* 4:a011338.

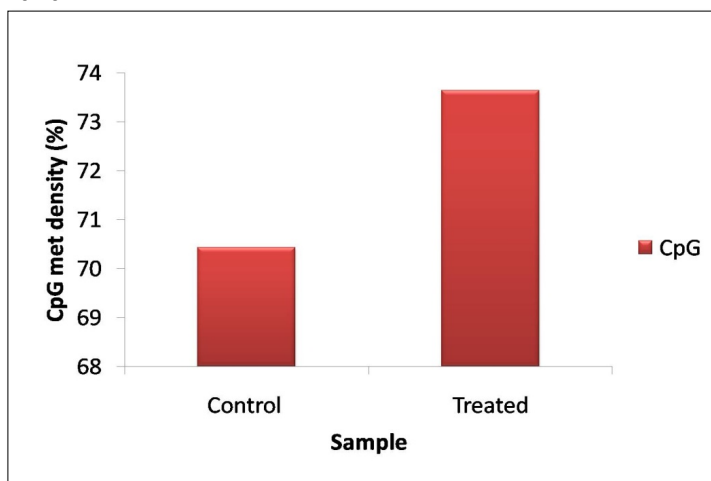
481 Narendra, D.P., Jin, S.M., Tanaka, A., Suen, D.F., Gautier, C.A., Shen, J., Cookson, M.R., and Youle R. (2010)
482 PINK1 is selectively stabilized on impaired mitochondria to activate Parkin. *PLoS Biol* 8:e1000298.

483 Noriyuki Matsuda KT (2015) The PARK2/Parkin receptor on damaged mitochondria revisited—uncovering the role
484 of phosphorylated ubiquitin chains. *Autophagy* 11:1700–1. doi: doi: 10.1080/15548627.2015.1071760.

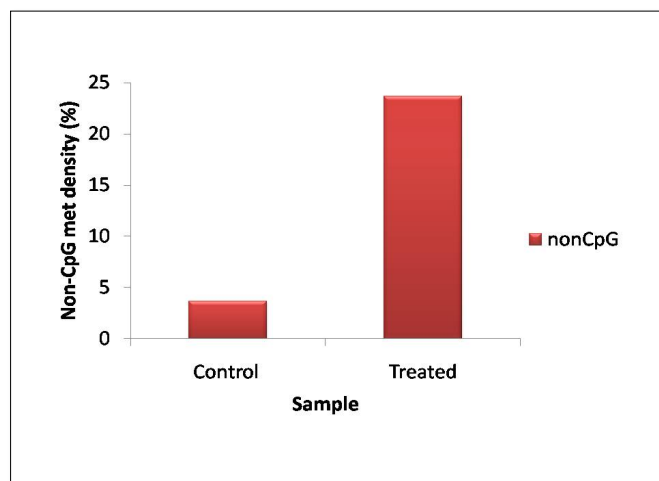
- 485 Orphanides G RD (2002) A unified theory of gene expression. *Cell* 108:439–51.
- 486 PA J (2012) Functions of DNA methylation: islands, start sites, gene bodies and beyond. *Nat Rev Genet* 13:484–
487 492.
- 488 Padmaja MV, Jayaraman M, Srinivasan AV, Srisailapathy CR RA (2012) PARK2 gene mutations in early onset
489 Parkinson’s disease patients of South India. *Neurosci Lett* 523:145–147.
- 490 Park JD, Chung YH, Kim CY, Ha CS, Yang SO KH et al (2007) Comparison of high MRI T1 signals with
491 manganese concentration in brains of cynomolgus monkeys after 8 months of stainless steel welding-fume
492 exposure. *Inhal Toxicol* 19:965–971.
- 493 Periquet M., Latouche M., Lohmann E., Rawal N., De Michele G., Ricard S., Teive H., Fraix V. VM and ND (2003)
494 Parkin mutations are frequent in patients with isolated early-onset parkinsonism. *Brain* 126:1271–1278.
- 495 Petit A, Kawarai T, Paitel E, Sanjo N, Maj M, Scheid M, Chen F, Gu Y, Hasegawa H, Salehi-Rad S, Wang L,
496 Rogava E, Fraser P, Robinson B, St George-Hyslop P TA (2005) Wild-type PINK1 prevents basal and
497 induced neuronal apoptosis, a protective effect abrogated by Parkinson disease-related mutations. *J Biol Chem*
498 280:34025–32.
- 499 Racette BA, Criswella SR, Lundinb JI, Hobsona A, Seixasb N, Kotzbauera PT, Evanoffc BA, Perlmuttera JS,
500 Zhangd J, Sheppardf L CH (2012) Increased risk of parkinsonism associated with welding exposure.
501 *Neurotoxicology* 33:1356–61. doi: .doi:10.1016/j.neuro.2012.08.011.
- 502 Rochet JC, Hay BA GM (2012) Molecular insights into Parkinson’s disease. *Prog Mol Biol Transl Sci* 107:125–88.
503 doi: doi: 10.1016/B978-0-12-385883-2.00011-4
- 504 Roede JR, Hansen JM, Young-Mi Go JD (2011) Maneb and Paraquat-Mediated Neurotoxicity: Involvement of
505 Peroxiredoxin/Thioredoxin System. *Toxicol Sci* 121:368–375. doi: doi:10.1093/toxsci/kfr058
- 506 Ryan Lister, Eran A. Mukamel, Joseph R. Nery, Mark Ulrich CAP, Nicholas D. Johnson, Jacinta Lucero, Yun
507 Huang, Andrew J. Dwork MD, Schultz, Miao Yu, Julian Tonti-Filippini, Holger Heyn, Shijun Hu JCW, et al
508 (2013) Global Epigenomic Reconfiguration During Mammalian Brain Development. *Science* (80-)
509 341:1237905–1237905.
- 510 Schapira (2008) Mitochondria in the aetiology and pathogenesis of Parkinson’s disease. *Lancet Neurol* 7:97–109.
- 511 Schnekenburger M TG and PA (2007) Chromium Cross-Links Histone Deacetylase 1-DNA Methyltransferase
512 Complexes to Chromatin, Inhibiting Histone-Remodeling Marks Critical for Transcriptional Activation. *Mol*
513 *Cell Biol* 7089–7101.
- 514 Settivari R, VanDuyn N, LeVora J NR (2013) The Nrf2/SKN-1-dependent glutathione S-transferase p homologue
515 GST-1 inhibits dopamine neuron degeneration in a *Caenorhabditis elegans* model of manganism.
516 *Neurotoxicology* 38:51–60.
- 517 Sharma R. PS. (2005) Toxic metals status in human blood and breast milk samples in an integrated steel plant
518 environment in central India. *Env Geochem Heal* 27:39–45.
- 519 Silvestri L, Caputo V, Bellacchio E, Atorino L, Dallapiccola B, Valente EM CG (2005) Mitochondrial import and
520 enzymatic activity of PINK1 mutants associated to recessive parkinsonism. *Hum Mol Genet* 14:3477–92.
- 521 Stephenson AP, Schneider JA, Nelson BC, Atha DH, Jain A, Soliman KF, Aschner M, Mazziro E RR (2013)
522 Manganese-Induced Oxidative DNA Damage in Neuronal SHSY5Y Cells: Attenuation of thymine base
523 lesions by glutathione and N-acetylcysteine. *Toxicol Lett* 218:299–307.
- 524 Susan Searles Nielsen, Harvey Checkoway, Susan R. Criswell FMF, Patricia L. Stapleton, Lianne Sheppard BAR
525 (2014) Inducible nitric oxide synthase gene methylation and parkinsonism in manganese exposed welders.
526 *Park Relat Disord*. doi: DOI: 10.1016/j.parkreldis.2015.01.007

- 527 Tamm C, Sabri F CS (2008) Mitochondrial-Mediated Apoptosis in Neural Stem Cells Exposed to Manganese.
528 *Toxicol Sci* 102:310–320.
- 529 Tarale P, Chakrabarti T, Sivanesan S, et al (2016) Potential Role of Epigenetic Mechanism in Manganese Induced
530 Neurotoxicity. *Biomed Res Int* 2016:1–18. doi: <http://dx.doi.org/10.1155/2016/2548792>
- 531 Trempe JF, Sauvé V, Grenier K, Seirafi M, Tang MY, Ménade M, Al-Abdul-Wahid S, Krett J, Wong K, Kozlov G,
532 Nagar B, Fon EA GK (2013) Structure of parkin reveals mechanisms for ubiquitin ligase activation. *Science*
533 (80-) 340:1451–5.
- 534 Wataru Satake, Yuko Nakabayashi, Ikuko Mizuta, Yushi Hirota, Chiyomi Ito, Michiaki Kubo, Takahisa Kawaguchi,
535 Tatsuhiko Tsunoda, Masahiko Watanabe, Atsushi Takeda, Hiroyuki Tomiyama, Kenji Nakashima, Kazuko
536 Hasegawa, Fumiya Obata, Takeo Yoshikawa, Hideshi YN& TT (2009) Genome-wide association study
537 identifies common variants at four loci as genetic risk factors for Parkinson’s disease. *Nat Genet* 41:1303–7.
- 538 WHO (2006) Guidelines for Drinking-Water Quality [electronic resource]: Incorporating First Addendum.
539 Available: http://www.who.int/water_sanitation_health/dwq/gdwq0506begin.pdf [accessed 26 January 2007].
- 540 Yang N, Wei Y, Wang T, Guo J, Sun Q, Hu Y, Yan X, Zhu X, Tang B1 XQ (2016) Genome-wide analysis of DNA
541 methylation during antagonism of DMOG to MnCl₂-induced cytotoxicity in the mouse substantia nigra. *Sci*
542 *Rep* 6:28933. doi: DOI: 10.1038/srep28933
- 543 Youle AMP and RJ (2014) The Roles of PINK1, Parkin, and Mitochondrial Fidelity in Parkinson’s Disease. *Neuron*
544 85:257–273.
- 545 Zhang D, Kanthasamy A, Anantharam V KA (2011) Effects of Manganese on Tyrosine Hydroxylase (TH) Activity
546 and TH-phosphorylation in a Dopaminergic Neural Cell Line. *Toxicol Appl Pharmacol* 254:65–71. doi:
547 doi:10.1016/j.taap.2010.03.023
- 548
- 549

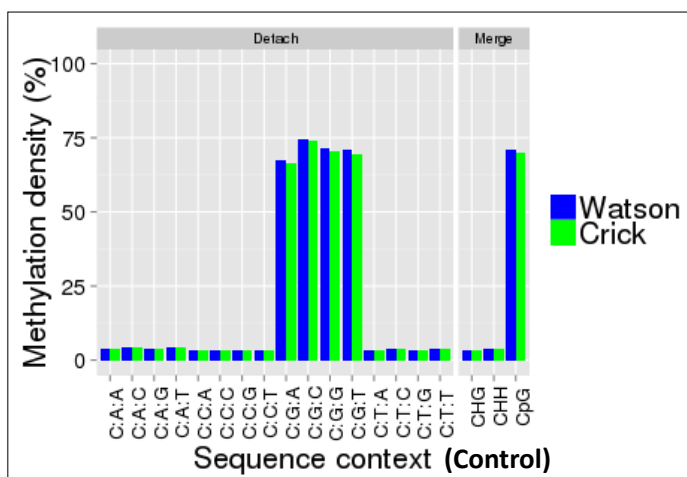
(A)



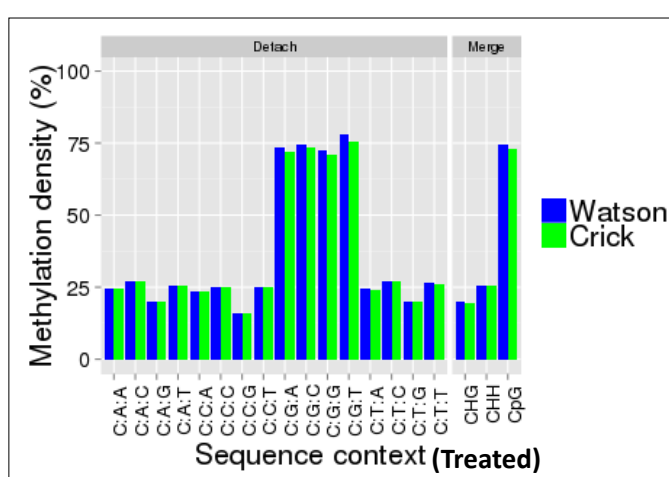
(B)



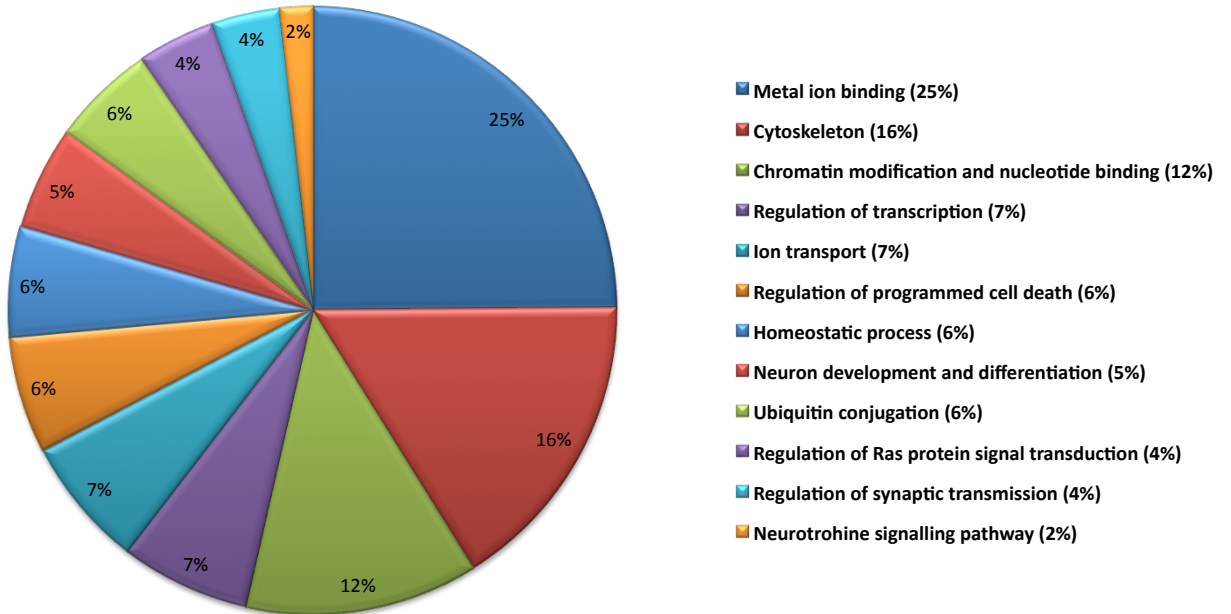
(C)



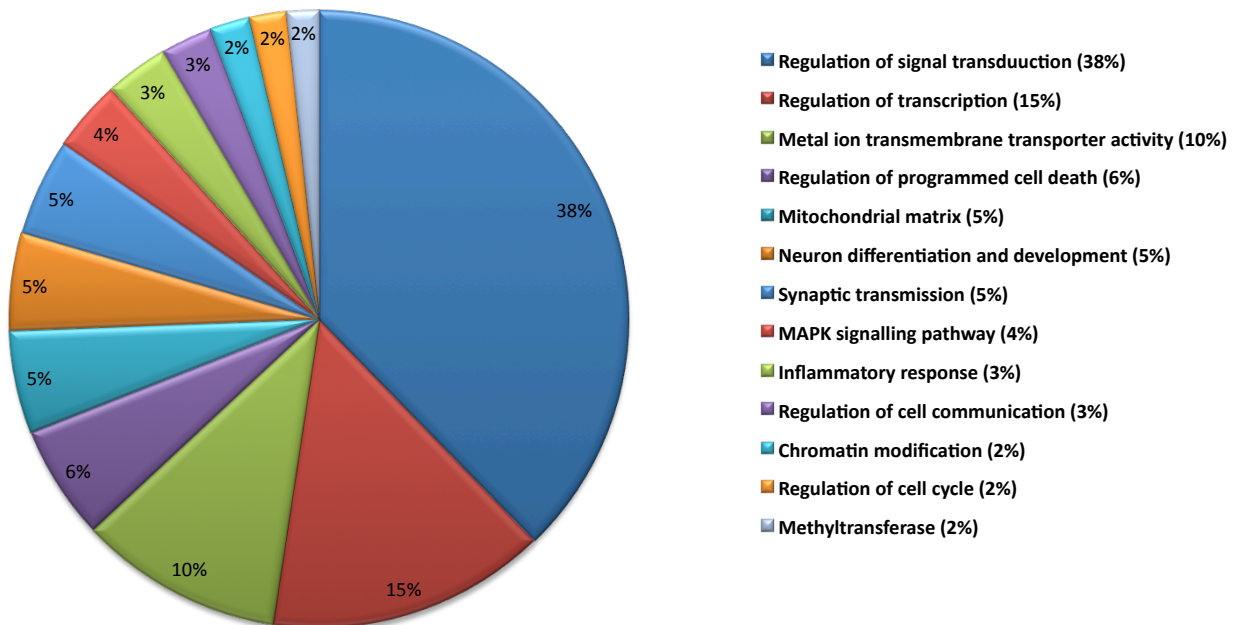
(D)

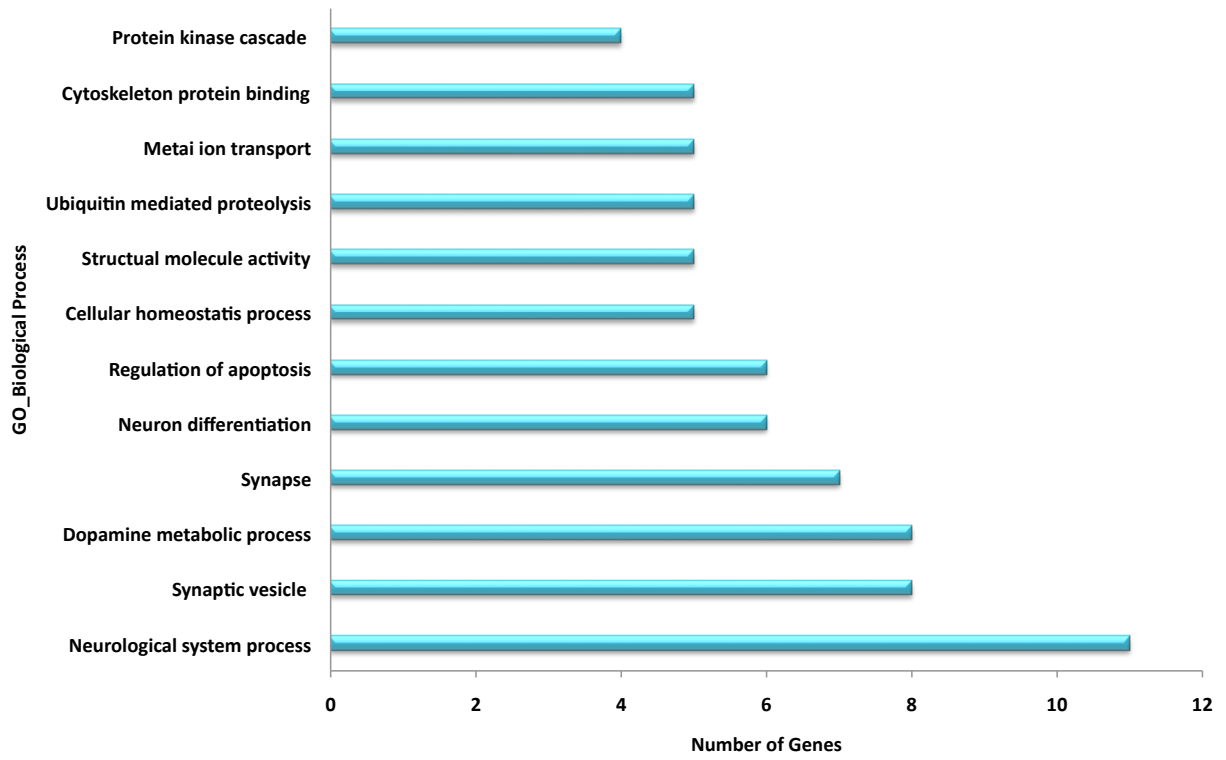


(A)



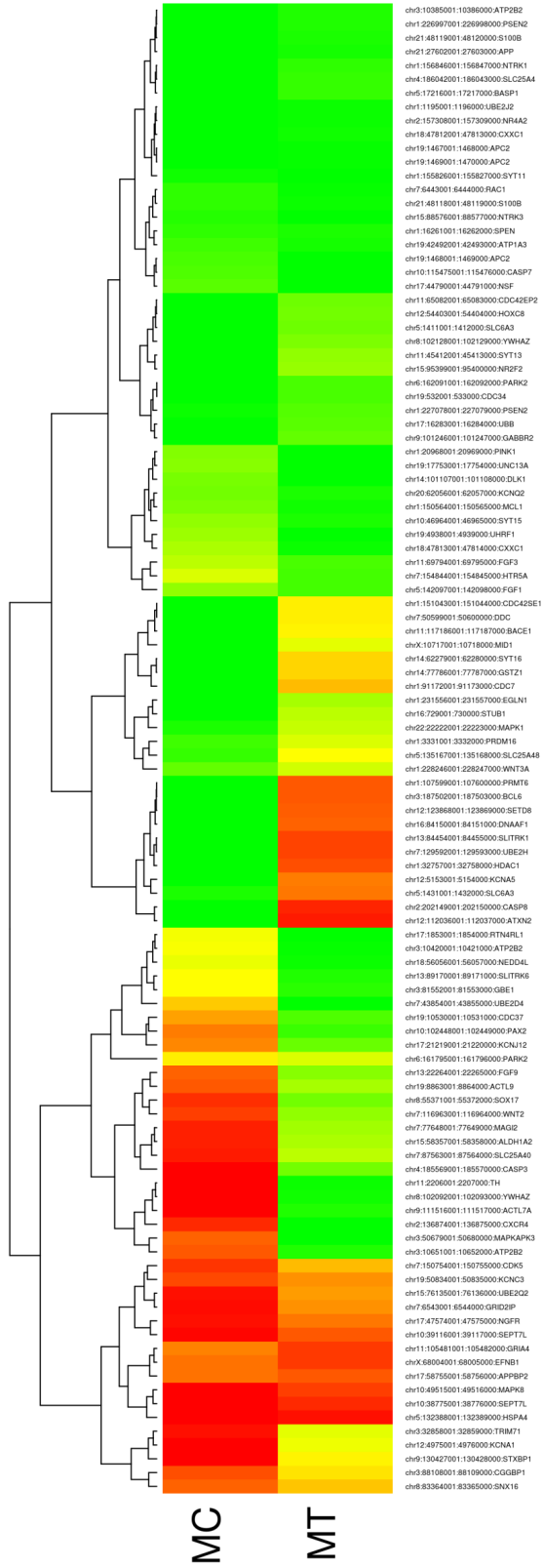
(B)

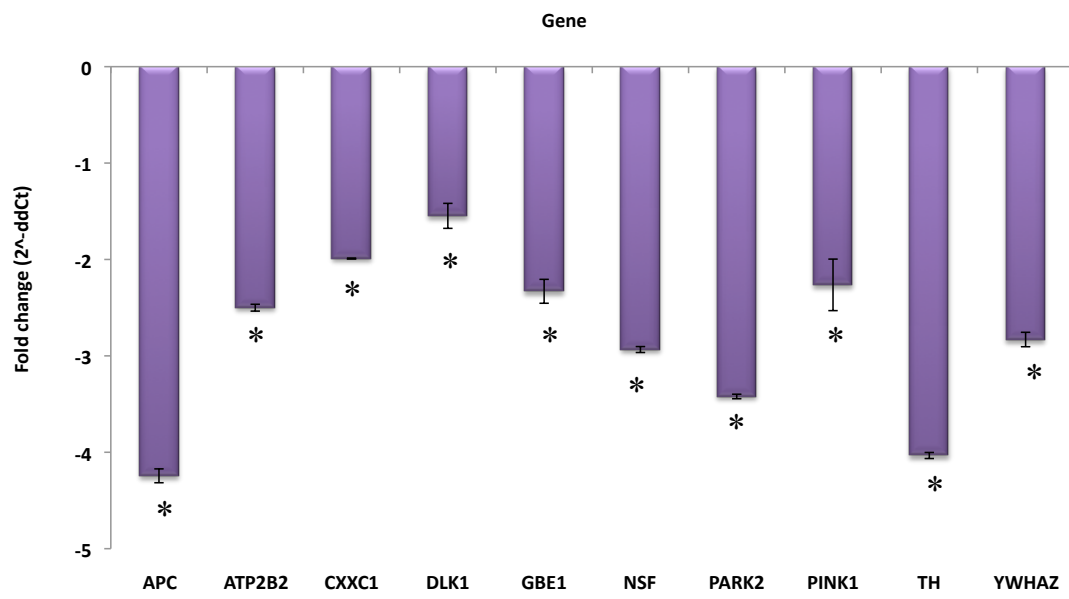


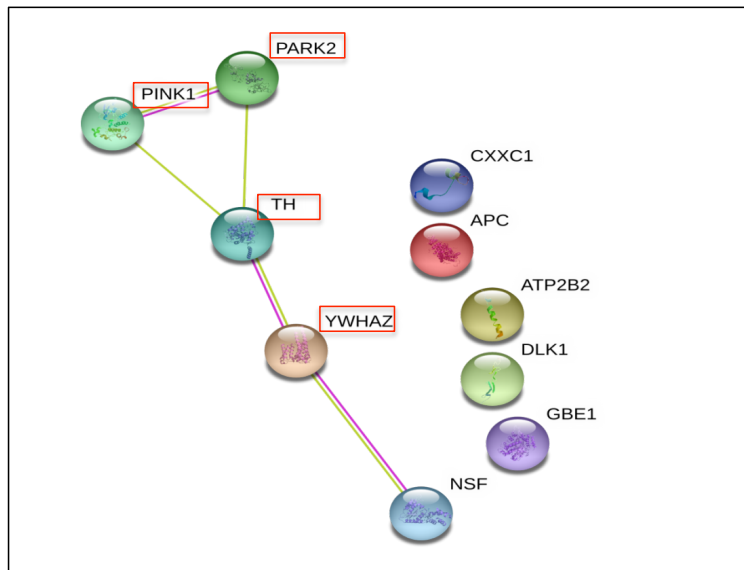




HeatMap







Network Stats

number of nodes: 10
 number of edges: 5
 average node degree: 1
 clustering coefficient: 0.833

expected number of edges: 1

PPI enrichment p-value: 0.000273

your network has significantly more interactions than expected (what does that mean?)

Functional enrichments in your network

Biological Process (GO)

pathway ID	pathway description	count in gene set	false discovery rate
GO:0071287	cellular response to manganese ion	2	0.0148
GO:1903204	negative regulation of oxidative stress-induced neuron death	2	0.0148
GO:1903377	negative regulation of oxidative stress-induced neuron intrinsic apoptotic signaling pathway	2	0.0148
GO:0001963	synaptic transmission, dopaminergic	2	0.0384
GO:0010042	response to manganese ion	2	0.0384
GO:0042415	norepinephrine metabolic process	2	0.0384
GO:0090140	regulation of mitochondrial fission	2	0.0384
GO:1903747	regulation of establishment of protein localization to mitochondrion	3	0.0385
GO:0014059	regulation of dopamine secretion	2	0.0452
GO:0043409	negative regulation of MAPK cascade	3	0.0452
GO:0009636	response to toxic substance	3	0.0484
GO:0097164	ammonium ion metabolic process	3	0.0484
GO:0097237	cellular response to toxic substance	2	0.0484
GO:1902176	negative regulation of oxidative stress-induced intrinsic apoptotic signaling pathway	2	0.0484
GO:1903827	regulation of cellular protein localization	4	0.0484

KEGG Pathways

pathway ID	pathway description	count in gene set	false discovery rate
05012	Parkinson s disease	3	0.0102